

## Prandtl-number dependence of turbulent flame propagation

Alan R. Kerstein

Combustion Research Facility, Sandia National Laboratories, Livermore, California 94551-0969

(Received 3 July 2001; published 26 November 2001)

Inertial-range cascade phenomenology is used to predict Prandtl-number (Pr) dependencies of turbulent flame properties. A unified picture of turbulent flame structure and burning velocity is developed that encompasses all Pr regimes. Implications of the analysis for gaseous flames (Pr near unity), autocatalytic fronts in liquids (high Pr), and astrophysical flames (low Pr) are noted.

DOI: 10.1103/PhysRevE.64.066306

PACS number(s): 47.27.Jv, 47.70.Fw, 47.27.Eq, 97.60.Bw

### I. INTRODUCTION

Propagation of reaction fronts in turbulent flow has been studied primarily in the context of gaseous flames, for which the Prandtl number (Pr) is near unity. The main properties of interest are the turbulent burning velocity, defined as the volume rate of reactant conversion per unit transverse area, and the local structure of the reaction fronts.

There are other turbulent reacting flows involving propagating fronts for which Pr is far from unity. Shy *et al.* showed that an aqueous autocatalytic reaction system is a useful experimental analog of gaseous combustion [1]. In fact, this high-Pr system provides a clearer validation of Damköhler's [2] theory of the transition from flamelet to distributed combustion than is achievable for gaseous combustion, owing to thermal expansion, radiative heat loss, and other complications in the latter case [3]. Low-Pr turbulent front propagation has not been studied experimentally, ostensibly due to practical difficulties and the absence of a strong motivation to study this regime.

However, there is an astrophysical low-Pr turbulent combustion process of timely interest, namely, the thermonuclear combustion in white dwarfs that is the presumed triggering mechanism for a class of supernova explosions [4]. This process has been of longstanding interest owing to its role in determining the elemental composition of matter. The recent use of supernovae as distance indicators in fundamental cosmological studies [5] has heightened interest in the empirical phenomenology of supernova behavior that is crucial to this application. Turbulent thermonuclear combustion is prominent among the poorly understood processes that are influential in this regard [6].

Models of astrophysical combustion can only be validated indirectly, if at all. One indirect approach to validation is extrapolation of known behaviors of terrestrially accessible combustion regimes. Analogies between gaseous combustion and thermonuclear combustion have been invoked for this purpose [6], but the nature of the implied Pr extrapolation has been considered only to a limited degree [7].

Establishment of quantitative connections among high-Pr liquid-phase autocatalysis, gaseous flames, and low-Pr astrophysical combustion processes faces significant obstacles owing to system-specific complications in each case. It is nevertheless useful to develop a conceptual framework encompassing all these regimes in order to provide a systematic basis for further investigation of this issue. Specifically, a

framework is sought that addresses the Pr dependence of two fundamental properties of propagating fronts in turbulence, the turbulent burning velocity and local flame structure.

### II. BURNING REGIMES AND TRANSITIONS

#### A. Assumptions

The turbulence and flame scalings assumed in the analysis are outlined. The turbulence is characterized by an integral scale  $L$  and a corresponding velocity  $U$  representing the magnitude of turbulent velocity fluctuations. These parameters and the kinematic viscosity  $\nu$  are combined to form a Reynolds number  $Re \equiv UL/\nu$ . The length scale  $\eta$  at which viscosity dissipates velocity fluctuations is assumed to obey the conventional Kolmogorov scaling  $\eta = Re^{-3/4}L$ . (Empirical coefficients of order unity are omitted from the scaling analysis.) The corresponding large-scale and dissipation-scale eddy-turnover times are  $T = L/U$  and  $t = \eta^2/\nu = Re^{-1/2}T$ , respectively. The laminar reacting front is characterized by a thermal diffusion coefficient  $\kappa = \nu/Pr$  and a chemical time scale  $\tau$ , from which the laminar flame speed  $S = (\kappa/\tau)^{1/2}$  and the laminar flame thickness  $\lambda = (\kappa\tau)^{1/2}$  are obtained. The diffusion coefficient, flame speed, and flame thickness can be modified by turbulence, as shown in the analysis.

The physical regimes of interest are conveniently parameterized by Pr and  $\lambda/\eta$ . This is not the most useful parameterization for other purposes, but conversion is straightforward.

The adoption of a single chemical parameter  $\tau$  that does not depend on local flow conditions excludes important real-world behaviors such as flame extinction and thermally diffusive flame instabilities [8]. Moreover, the application of conventional inertial-range cascade phenomenology to turbulent combustion is not guaranteed to be correct in principle. In particular, an analysis of turbulent combustion predicated on the dominance of intermittency effects relative to the mean-field scalings used here yields results that differ in some respects from the results of the present analysis [9]. The present goal is to establish the simplest possible baseline for the interpretation of Pr effects on turbulent flame propagation, and thereby to identify directions for future research that may lead to an improved theoretical picture.

#### B. Turbulent burning velocity

In Sec. II A, the laminar flame speed is expressed in terms of a transport coefficient and a time scale. The turbulent

burning velocity  $u_T$  can be formulated analogously, using the turbulent transport coefficient  $\kappa_e = UL$  (here assuming  $\kappa_e > \kappa$ ) and the rate-limiting time scale for turbulent combustion. The governing time scales are the large-scale time  $T$ , which is the rate-limiting advective time scale for fuel entrainment into the flame brush and subsequent scale reduction, and the chemical time scale  $\tau$ . Therefore

$$u_T = (\kappa_e/T)^{1/2} = U, \quad (2.1)$$

for  $T \geq \tau$  and

$$u_T = (\kappa_e/\tau)^{1/2} = (\kappa_e/\kappa)^{1/2} S = (\text{Re Pr})^{1/2} S, \quad (2.2)$$

for  $\tau > T$ . The crossover between burning-rate regimes thus occurs at  $\tau = T$ , or in the preferred parameterization,  $\text{Pr} = \text{Re}^{1/2} (\lambda/\eta)^{-2}$ .

Equation (2.1) reflects the fact that there is a unique large-scale quantity  $U$  with dimensions of velocity, so  $u_T$  must scale as  $U$  unless some small-scale process affects the overall fuel conversion rate. Equation (2.2) corresponds to the latter situation, for which advective homogenization is faster than chemical conversion.

If  $\kappa_e < \kappa$  (i.e., molecular transport dominates turbulent transport), then advective processes are irrelevant and  $u_T = S$ . This case corresponds to  $\text{Pr} < 1/\text{Re}$ . For this regime, small corrections to the relation  $u_T = S$  due to flame perturbation by eddies much larger than  $\lambda$  have been analyzed [8,10], but they are not considered here.

Equations (2.1) and (2.2) correspond to the Huygens propagation (HP) and distributed reaction zone (DRZ) regimes originally proposed by Damköhler [2], who identified these regimes with the limits  $\lambda \ll L$  and  $\lambda \gg L$ , respectively. Various criteria for the onset of the DRZ regime have been proposed [11,12]. Ronney *et al.* found that the criterion  $\tau > t$  was consistent with their experimental observations of the onset of DRZ scaling of  $u_T$  [3], but the experiments were performed at  $\text{Re}$  low enough so that the results do not conclusively discriminate between this criterion and the criterion  $\tau > T$  proposed here. The rationale for the criterion  $\tau > T$  is discussed further in Sec. III A.

### C. Transition to stirred flames

It is proposed that local reaction-front structure undergoes a transition that is distinct from the burning-velocity transition analyzed in Sec. II B. The flamelet regime, in which turbulence advects reaction fronts without major modification of reaction-front structure, is widely recognized and well understood [8,12]. Also recognized, but less well characterized with regard to properties and conditions for onset, is the burning regime in which turbulence strongly modifies reaction-front structure. Here this regime is denoted the stirred-flame regime, a terminology chosen in order to distinguish it from the DRZ burning-velocity regime analyzed in Sec. II B.

One goal of the present study is to define the distinction and analyze its consequences. The burning-velocity transition criterion used in the interpretation of high- $\text{Pr}$  measure-

ments implies no distinction between these regimes [3], but the present analysis yields a different conclusion.

The transition from flamelet to stirred-flame structure is considered first. The nature of the stirred-flame regime in comparison to the DRZ regime is considered in Sec. III A. Details of the transition from flamelet to stirred-flame structure depend on whether  $\lambda$  or  $\eta$  is larger, so the two cases are considered individually.

For  $\lambda < \eta$ , individual flamelets are subject to strain by the smallest eddies, but individual eddies are not contained within the reaction zone. This strain can disrupt the laminar flame structure if it is strong enough to narrow individual lamellae of combustion products faster than they widen by flame propagation. This narrowing would ultimately cause back-to-back pairs of outward-propagating flames to merge and possibly extinguish. (Extinction reflects dependence of  $\tau$  on local conditions and therefore, is beyond the scope of the present analysis, see Sec. V.) The condition for this flame disruption is that a size- $\lambda$  slab experiences strain narrowing that exceeds propagative broadening, i.e.,  $\lambda/t > S$ . This is equivalent to requiring  $\tau > t$ .

The relation  $\tau > t$  gives  $\text{Pr} > (\lambda/\eta)^{-2}$ . Thus, the breakdown of laminar flame structure for  $\lambda < \eta$  occurs at  $\text{Pr} > 1$ .

The strain-induced narrowing leading to flame merger ultimately causes flame broadening, as follows. By volume conservation, the strain that narrows product lamellae commensurately increases the total area of the flame surface, which, therefore, becomes increasingly wrinkled within a given volume of the flame brush. Therefore, the fuel lamellae separating flames are likewise narrowed, so that fuel and product lamellae eventually coexist within size- $\lambda$  regions. In effect, the strongly wrinkled reaction surface is homogenized to form a distributed reaction zone. (For  $\tau < t$ , the fuel is consumed before homogenization occurs.) Assuming that reaction zones at least as large as  $\eta$  are formed, additional flame broadening by eddy diffusivity can occur, as explained in Sec. III A. Indirect evidence of this mechanism is the observation of a DRZ combustion regime in high- $\text{Pr}$  reaction-front propagation [3], implying that the reaction zone may broaden to encompass the entire flame brush (though this does not necessarily occur, see Sec. III A).

For  $\lambda > \eta$ , turbulent eddies ranging in size from  $\eta$  to  $\lambda$  are contained within the reaction zone. The criterion for disruption of the laminar flame structure by these eddies is that their contribution to transport dominates molecular transport. Inertial-range eddy diffusivity is an increasing function of eddy size, so this criterion is applied by comparing transport by size- $\lambda$  eddies to  $\kappa$ . The eddy diffusivity of a size- $\lambda$  eddy, denoted  $\kappa_\lambda$ , is governed by the inertial-range scaling  $\kappa_\lambda = (\lambda/\eta)^{4/3} \nu$ . The disruption criterion is then  $\kappa_\lambda > \kappa$ , which gives  $\text{Pr} > (\lambda/\eta)^{-4/3}$ . The same result is obtained by requiring the chemical time  $\tau$  to be larger than the turnover time  $t_\lambda = (\lambda/\eta)^{2/3} t$  of a size- $\lambda$  eddy, which is the criterion for the onset of strain-induced narrowing due to eddies larger than  $\lambda$ . Because  $\lambda > \eta$  has been assumed, the transition induced by size- $\lambda$  eddies occurs at  $\text{Pr} < 1$ .

The results so far can be summarized as follows. Flamelet structure is obtained  $\tau < t_s$ , where  $t_s$  is the turnover time of the eddy of size  $\max(\eta, \lambda)$ . Stirred-flame structure is obtained

for  $t_s < \tau < T$ .  $\tau > T$  corresponds to the DRZ regime discussed in Sec. II B. The crossover from flamelet to stirred-flame structure is initiated by distinct mechanisms at high and low Pr. For Pr=1, the crossover condition  $\tau/t=1$  is equivalent to  $\lambda/\eta=1$ . For this case, these two equivalent thresholds for transition to stirred-flame structure are well known in the combustion literature [12], where  $\tau/t$  is called the turbulent Karlovitz number.

### III. FLAME STRUCTURE

#### A. Thickness of stirred flames

Details of flame structure are examined for the two structural regimes that have been identified. Two structural characteristics are considered, flame thickness (in this section) and curvature (in Sec. III B). Also, the analysis of flame thickness provides further insight into the burning-velocity regimes identified in Sec. II B.

The physics determining the thickness of stirred flames is closely related to the mechanism governing the transition to stirred flames. In the stirred-flame regime, it is proposed in Sec. II C that either the undisturbed flame is thicker than the Kolmogorov scale  $\eta$  or else flame-surface wrinkling causes homogenization within zones at least as large as  $\eta$ .

Either scenario implies an effective flame thickness  $l_f$  that is at least as large as  $\eta$ . For given  $l$ , consider whether eddies of size  $l$  induce further flame thickening. A simple criterion is obtained by comparing the speed  $S_l$  of the thickened flame to the eddy velocity  $v_l=l/t_l$ , where  $t_l=(l/\eta)^{2/3}t$  is the turnover time of a size- $l$  eddy. If  $S_l > v_l$ , then the flame traverses a size- $l$  eddy before the eddy turns over, so size- $l$  eddies are effectively frozen with respect to front propagation. (See Sec. III B for another application of this reasoning.) Therefore, size- $l$  eddies contribute to flame thickening only if  $S_l < v_l$ . Based on the relations  $S_l=(\kappa_l/\tau)^{1/2}$  and  $\kappa_l=l v_l$ , the condition for flame thickening is  $t_l < \tau$ .

Therefore, the flame is thickened to a size  $l=l_f$  determined by the condition  $t_l=\tau$ , giving  $l_f=(\tau/t)^{3/2}\eta=(\tau/T)^{3/2}L$ . This scaling, and the physical picture on which it is based, have been noted previously [12–15]. The corresponding value of  $S_l$  is  $S_f=(\tau/T)^{1/2}U$ .

For  $\tau < T$ , the thickened flame is thus characterized by a thickness  $l_f < L$  and a speed  $S_f < U$ . From the perspective of large-scale processes, the thickened flame is functionally equivalent under these conditions to a laminar flame, with  $l_f$  and  $S_f$  corresponding to laminar properties  $\lambda$  and  $S$ , respectively. Accordingly, Eq. (2.1) governing the burning velocity in the flamelet regime is again applicable. This explains why the condition  $\tau > T$ , rather than  $\tau > t$ , is proposed here as the criterion for crossover to the DRZ burning regime, Eq. (2.2).

#### B. Flame curvature

In Sec. III A, the effective speed  $S_l$  of a thickened flame is compared to the eddy velocity  $v_l$  to determine whether size- $l$  eddies contribute to flame broadening or are effectively frozen from the viewpoint of the flame. This velocity comparison was originally introduced in an analysis of the flame-

let regime in order to determine the finest scale of flame front wrinkling, denoted the Gibson scale  $l_g$  [12]. The condition  $S=v_l$  gives

$$l_g=(S/U)^3L, \quad (3.1)$$

valid for  $S > v_\eta$ . This scale also characterizes the front curvature radius in the flamelet regime.

$l_g$  can exceed  $\eta$  only if  $S > v_\eta$ . This condition can be expressed as  $\text{Pr} < (\lambda/\eta)^{-1}$ . If Pr doesn't obey this equality, then all eddies can wrinkle the flame. In this case, flame curvature is determined by different mechanisms depending on whether  $\lambda$  or  $\eta$  is larger.

For  $\lambda < \eta$ , Kolmogorov strain exponentially increases flame-surface area [16], with a corresponding exponential decrease of curvature radius  $r$ . Introducing a notional time coordinate  $\theta$ , this implies  $r/\eta=\exp(-c\theta/t)$ , where  $c$  is an unknown numerical coefficient. As  $\theta$  increases and  $r$  decreases, the ratio  $r/\theta$  decreases until  $r/\theta=S$ . While  $r/\theta$  exceeds  $S$ , only a small fraction of the fuel is consumed. When  $r/\theta$  falls below  $S$ , flame propagation consumes the (size- $r$ ) fuel zones before significant additional wrinkling occurs. Therefore, the condition  $\theta=r/S$  is inserted into the expression for  $r(\theta)$  to obtain the balance condition

$$r/\eta=\exp[-cr/(St)], \quad (3.2)$$

a transcendental equation that determines  $r$ .

Two limiting cases are noted.  $r=\lambda$  is the condition for crossover to stirred flames. This requires  $\tau$  to be of order  $t$  unless  $\lambda$  is exponentially small compared to  $\eta$ . This is the crossover condition obtained in Sec. II C by a method involving less detailed analysis of advected-flame kinematics.  $r=\eta$  corresponds to balance between flame propagation and the Kolmogorov velocity  $v_\eta$ , thus marking the onset of Gibson scaling  $r=l_g$ , where  $l_g$  is given by Eq. (3.1).

For  $\lambda > \eta$ , the flamelet criterion is  $\tau < t_\lambda$ , or equivalently,  $S > v_\lambda$ . The latter relation implies that  $l_g > \lambda$ . Again,  $r$  is governed by Gibson scaling.

In the stirred-flame regime, the flame thickness and flame curvature radius obey equivalent scalings because both are governed by the eddy whose velocity matches the speed of the thickened flame. Thus, flame curvature is distinguished from flame thickness only in the flamelet regime.

#### C. Property fluctuations

A complete characterization of flame structure must encompass additional details of internal flame structure as well as the thickness and curvature scalings considered so far. In the flamelet regime, individual flame zones have an essentially undisturbed laminar structure that is well described by laminar flame theory [8]. The internal structure of thickened flames reflects the coupled influences of chemical reaction and turbulent advection.

As noted in Sec. III A, the flame thickness  $l_f$  in the latter case is determined by the condition  $t_l=\tau$ . Accordingly, eddies smaller than  $l_f$  within the thickened flame correspond to time scales shorter than  $\tau$ . Therefore, they cascade property fluctuations at scale  $l_f$  to smaller scales without significant

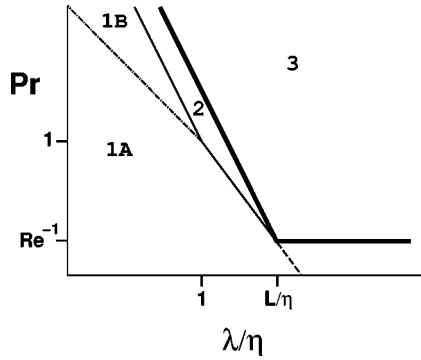


FIG. 1. Regimes of turbulent flame structure and burning velocity, plotted in logarithmic coordinates: 1, flamelet regime; 2, stirred-flame regime; 3, distributed reaction zone (DRZ) burning-velocity regime. The Huygens propagation (HP) burning-velocity regime consists of flame-structure regimes 1 and 2. The boundary between regions 1 and 2 (flame-structure transition) is  $Pr = (\lambda/\eta)^{-2}$  for  $\lambda < \eta$  and  $Pr = (\lambda/\eta)^{-4/3}$  for  $\eta < \lambda < L$ , where  $L$  is the turbulence integral scale,  $\eta$  is the viscous dissipation scale, and  $\lambda$  is the laminar flame thickness. The boundary between regions 2 and 3 (burning-velocity transition) is  $Pr = Re^{1/2}(\lambda/\eta)^{-2}$ . As  $Re$  varies, the boundary of region 3 (thick line) shifts, with the vertex of this boundary traversing the boundary between regions 1 and 2 (thin solid line; dashed line indicates the extrapolation of this boundary for increasing  $Re$ ). Also shown is the partition of region 1 into subregions 1A and 1B in which the flame curvature radius is governed by Gibson scaling, Eq. (3.1), and an alternative scaling, Eq. (3.2), respectively. The boundary between these subregions is  $Pr = (\lambda/\eta)^{-1}$ , restricted to  $\lambda < \eta$  (dot-dashed line).

chemical change during the cascade process.

The typical variation of thermochemical properties at the scale  $l_f$  corresponding to the flame thickness is the difference between the unburned (fuel) and burned (product) states of the fluid. The typical property fluctuation across a distance  $l < l_f$  is governed, to leading order, by the spectral theory of the turbulent cascade of a passive scalar. (Deviations from this theory may arise because the scalars are not chemically passive;  $t_l/\tau$  is finite, though small.)

The phenomenology of the passive scalar cascade is well documented [17] and therefore, is not presented here. However, one nuance concerning this cascade is noted. The generally accepted picture of the low- $Pr$  cascade structure [17] is difficult to test empirically. The available experimental and numerical simulation results [18,19] admit the possibility of alternative interpretations whose impact at the very low  $Pr$  values of astrophysical interest could be significant.

#### IV. PHASE DIAGRAM

The crossover scalings that have been obtained are illustrated graphically in the phase diagram shown in Fig. 1. One feature of the diagram is that the burning-velocity transition boundary and the flame-structure transition boundary intersect where  $\lambda = L$ . To the right of that point is a region in which turbulent eddies of all sizes are contained within the flamelet reaction zone. The criterion for turbulence effects on flame propagation is then  $\kappa_e > \kappa$ , giving  $Pr > 1/Re$ . There is no independent time-scale criterion in this regime because

individual straining motions are not large enough to distort flame structure. Only the collective effect of eddies, represented by  $\kappa_e$ , can affect the flame. For  $Pr < 1/Re$ , the effect of turbulence on flame structure is negligible.

With this extension to  $\lambda > L$ , the phase diagram describes all of the parameter space. The sketch corresponds to a particular value of  $Re$ . Strictly speaking, the phase diagram lives in a three-parameter space corresponding to the family of diagrams obtained by displacing the thick boundary so that its vertex moves along the boundary corresponding to the low- $Pr$  flame-structure transition (extrapolated by the dashed line to indicate the vertex trajectory in the direction of increasing  $Re$ ).

The parameterization used in this analysis was selected because it allows the concise representation of burning regimes that is illustrated in Fig. 1. Previous empirically based studies recognized  $\lambda/\eta$  as a key parameter governing turbulent flame transitions [20]. It should be noted, however, that the current parameterization is not particularly convenient for examining turbulence sensitivities for fixed flame properties, or vice versa. Conversion to parameterizations that are more convenient for these purposes is straightforward.

The abrupt slope change of the boundary between regions 1 and 2 at  $Pr = 1$  is an idealization. For real physical systems, the slope would change gradually in the vicinity of  $Pr = 1$ . Therefore, the transition from flamelet to stirred-flame reaction-zone structure is particularly dependent on system-specific details for  $Pr$  near unity.

#### V. DISCUSSION

Despite the long history of turbulent combustion research [8,12,21], there is not yet a complete, validated picture of combustion regime scalings and the crossovers among them. Fifty five years after Damköhler laid the conceptual foundations of the subject, Ronney *et al.* provided the first quantitative demonstration of the crossover between burning-velocity regimes [3].

It is revealing that this was achieved using a liquid-phase autocatalytic system rather than a combustion process. This indicates the efficacy of studying physical analogs rather than combustion *per se* in order to elucidate the underlying physics of turbulent combustion.

For  $Pr$  near unity, it has been noted that flame structure is particularly sensitive to system-specific details. To clarify the underlying physical principles, it is therefore useful to study combustion analogs with  $Pr$  far from unity.

In addition to  $Pr$  considerations, gaseous combustion is subject to further complications that obscure the physics considered here. The multistep nature and thermal sensitivity of combustion chemistry causes  $\tau$  to depend on local conditions, modifying parameter dependencies and introducing new phenomena such as flame extinction [8]. Also, laminar flame fronts consist of preheat and reaction zones of different widths that respond differently to turbulent strain, introducing complications not reflected in the adoption of a single laminar front thickness  $\lambda$  [12]. The difficulty of interpreting measured turbulent flame behaviors has been exacerbated by these complications and by the lack, until the recent liquid-

phase studies [1,3], of alternate pathways to the underlying physics.

Although the liquid-phase study of the HP-DRZ transition [3] is a significant step forward, it leaves some important questions unresolved. For this experiment,  $Pr$  is of order  $10^3$ . [Strictly speaking, this is the value of the Schmidt number ( $Sc$ ) rather than  $Pr$  because propagation involved species rather than heat transport in this experiment.] To satisfy the flamelet criterion  $\lambda < \eta Pr^{-1/2}$  for  $Pr$  this high, reaction fronts must be two orders of magnitude thinner than the Kolmogorov microscale. To satisfy this stringent requirement in a practical flow configuration, fronts thinner than the spatial resolution of the imaging system were required. Therefore, the presumed flamelet nature of the propagation regime could not be verified. Another limitation of the experiment was that the flow  $Re$  was low enough so that the results do not discriminate between proposed alternative scalings (Sec. II B).

To gain additional information using this reaction process, the experiment would have to be scaled up considerably, both to increase  $Re$  and to allow spatially resolved imaging of reaction fronts. This scale-up would be costly but could be worthwhile in view of its likely contribution to fundamental understanding of turbulent combustion.

An alternate approach that might be more cost effective would be to use a reaction system that provides comparable information while imposing less stringent experimental requirements. A liquid-phase exothermic process in which heat rather than a product species is the catalytic agent is one possibility. In liquids,  $Pr$  is order 10, large enough for exploration of high- $Pr$  behavior but much smaller than typical  $Sc$  values. This would allow flamelet behavior for larger flame thicknesses (relative to  $\eta$ ) than in the reaction system using chemical autocatalysis.

Liquid-phase experiments have two advantages relative to gas-phase experiments. First,  $Pr$  is far from unity, avoiding complications specific to near-unity  $Pr$ . Second, liquids have low coefficients of thermal expansion, reducing disturbance of the flow field by the reaction process. Thermal expansion effects can obscure the underlying scalings and in fact, may cause the turbulent combustion process to be inherently tran-

sient and, therefore, not amenable to any sort of quasisteady analysis [22]. These effects might be reduced in the gas phase by using a fuel with a low heat of combustion. However, the constraint on the heat of combustion would be more stringent than for liquids owing to the higher thermal expansion coefficient of gases. It may be difficult to formulate a suitable gaseous fuel.

The low- $Pr$  regime could be investigated using a metallic liquid fuel. Imaging would be precluded, but time-resolved single-point measurements in metallic liquids are feasible and can provide useful information [23].

One reason for seeking better understanding of the crossover from flamelets to stirred flames, distinct from any connection to  $u_T$  scaling, is the role of flame broadening in establishing the preconditions for a deflagration-to-detonation transition (DDT). DDT in gaseous flames is often preceded by flame quenching, which is not considered in the present analysis. In the detonation scenario for supernova explosion, DDT preconditioning may be substantially different. Thermonuclear flames are relatively resistant to quenching [24] and  $Pr$  in these flames is as low as  $10^{-5}$  [25]. Evaluation of the likelihood that detonation, rather than self-accelerated deflagration, is the explosion mechanism is currently based largely on analogies to gas-phase studies [6]. In view of the  $Pr$  and other sensitivities noted here, a low- $Pr$  experiment might provide information of more direct relevance to stellar conditions.

In summary, there are important fundamental and practical reasons for adopting an integrated view of turbulent combustion over the entire range of relevant  $Pr$  values, which spans at least eight orders of magnitude. Validation of the conceptual framework proposed here may enable  $Pr$  extrapolations that provide insight into complicated practical problems through the study of simpler physical analogs.

#### ACKNOWLEDGMENTS

The author would like to thank Adam Oberman for discussions that motivated this work and Forman Williams for helpful comments. Support from the Division of Chemical Sciences, Geosciences, & Biosciences, Office of Science, U.S. Department of Energy is acknowledged.

- 
- [1] S.S. Shy, R.H. Jang, and P.D. Ronney, *Combust. Sci. Technol.* **114**, 329 (1996).
  - [2] G. Damköhler, *Z. Elektrochem. Angew. Phys. Chem.* **46**, 601 (1940).
  - [3] P.D. Ronney, B.D. Haslam, and N.O. Rhys, *Phys. Rev. Lett.* **74**, 3804 (1995).
  - [4] S.E. Woosley and T.A. Weaver, *Astrophys. J.* **423**, 371 (1994).
  - [5] S. Perlmutter *et al.*, *Astrophys. J.* **517**, 565 (1999).
  - [6] W. Hillebrandt and J.C. Niemeyer, *Annu. Rev. Astron. Astrophys.* **38**, 191 (2000).
  - [7] J.C. Niemeyer and A.R. Kerstein, *New Astron.* **2**, 239 (1997).
  - [8] F. A. Williams, *Combustion Theory*, 2nd ed. (Benjamin/Cummings, Menlo Park, 1985).
  - [9] M. Chertkov and V. Yakhot, *Phys. Rev. Lett.* **80**, 2837 (1998).
  - [10] A.R. Kerstein and W.T. Ashurst, *Phys. Rev. Lett.* **68**, 934 (1992).
  - [11] F.A. Williams, *J. Fluid Mech.* **40**, 401 (1970).
  - [12] N. Peters, *Turbulent Combustion* (Cambridge University Press, Cambridge, 2000).
  - [13] V.L. Zimont, *Combust. Explos. Shock Waves* **15**, 305 (1979).
  - [14] P.D. Ronney and V. Yakhot, *Combust. Sci. Technol.* **86**, 31 (1992).
  - [15] N. Peters, *J. Fluid Mech.* **384**, 107 (1999).
  - [16] S.S. Girimaji and S.B. Pope, *J. Fluid Mech.* **220**, 427 (1990).
  - [17] M. Lesieur, *Turbulence in Fluids*, 3rd ed. (Kluwer, Dordrecht, 1997).
  - [18] C.H. Gibson, W.T. Ashurst, and A.R. Kerstein, *J. Fluid Mech.* **194**, 261 (1988).

- [19] J.R. Chasnov, *Phys. Fluids A* **3**, 1164 (1991).
- [20] D.R. Ballal and A.H. Lefebvre, *Proc. R. Soc. London, Ser. A* **344**, 217 (1975).
- [21] B. Lewis and G. von Elbe, *Combustion, Flames, and Explosions of Gases*, 2nd ed. (Academic Press, New York, 1961).
- [22] A.R. Kerstein, *Combust. Sci. Technol.* **118**, 189 (1996).
- [23] L.L. Eyler and A. Sesonske, *Int. J. Heat Mass Transf.* **23**, 1561 (1980).
- [24] J.C. Niemeyer, *Astrophys. J. Lett.* **523**, L57 (1999).
- [25] R. Nandkumar and C.J. Pethick, *Mon. Not. R. Astron. Soc.* **209**, 511 (1984).